Volume : 1 | Issue : 3 | December 2011 ISSN - 2249-555X

Research Paper Electronics

Analyzing a Brushless DC motor with a Fuzzy Logic Controller using MATLAB/SIMULINK

* G Prasad **Raees Unnisa
***Dr. P. V. N. Prasad ****Dr. G. Tulasi Ram Das

* Assistant Prof., Dept. of Electrical and Electronics Engg., GITAM University, Visakhapatnam,

** Department of Electrical and Electronics Engineering, GITAM University, Visakhapatnam

*** Professor, Dept. of Electrical and Electronics Engg., College of Engg., Osmania University

**** Professor, Department of Electrical and Electronics Engg, College of Engg., JNTUH

ABSTRACT

Brushless DC Motors are rotating electric machines which convert electrical energy into mechanical power. Brushless DC Motors (BLDC Motors), also known as Electronically Commuted motors are synchronous electric motors powered by DC electricity and having electronic commutation system, rather than mechanical commutators and brushes. The modeling of BLDC motor involves two loops. The first is the current control loop and the second is the speed control loop. The analysis of the BLDC motor is based on the simulation results of the speed control block, current control block and Voltage Source Inverter (VSI). Hence an advanced simulation model for BLDC motor drives using MATLAB can be presented. In this developed model, the dynamic characteristics of speed and torque as well as voltages and currents can be efficiently monitored and analyzed. A Fuzzy Logic Controller (FLC) here involves two inputs and a output. The difference between the reference speed and the actual speed gives the error. MATLAB/Fuzzy logic toolbox is used to simulate FLC which can be integrated into simulations with Simulink. Hence, the control algorithms for fuzzy logic and PID are compared. Also, the dynamic characteristics of the BLDC motor as well as currents and voltages of the inverter components are easily observed and analyzed by using the developed model.

Keywords : BLDC Motor, Electronically commutated motors, Fuzzy logic controller

Introduction

Brushless DC (BLDC) motors are rotating electrical machines which convert Electrical energy into mechanical energy. As the name implies, BLDC motors do not use brushes for commutation instead they are electronically commuted. BLDC motors have many advantages over brushed DC motors and induction motors, a few of these are:

a. Better speed Vs torque characteristics
b. High dynamic response
c. High efficiency
d. Long operating life
e. Noiseless operation
f. Higher speed ranges

Before now, several simulation models have been proposed for the analysis of BLDC motors drives. These models are based on state-space equations, Fourier series, and the d-q axis model. In this paper we propose a simulation model with fuzzy logic controller for an entire BLDC motor drive and its actual implementation. In this model the trapezoidal back EMF waveforms are modeled as a function of rotor position and the switching function concept is adopted to model the Voltage source inverter (VSI). This in turn results in obtaining the detailed voltage and current waveforms of the inverter. MATLAB/fuzzy logic toolbox is used to design FLC, which is integrated into simulations with Simulink.

Therefore, it can be expected that the developed simulation model can be an easy-to-design tool for the development of BLDC motor drives including control algorithms and topological variations with reduced computation time.

Analysis Of Bldc Motor Drive System

Figure 1 shows the overall system configuration of the three-phase BLDC motor drive. The PWM inverter topology is a six-switch voltage-source configuration with constant dc-link voltage (Vd), which is identical with the induction motor drives and the permanent magnet ac motor drives. The analysis is based on the following assumption for simplification:

a. The motor is saturated.
b. Stator resistances of the all the windings are equal, and self-and mutual inductances are constant.
c. Power semiconductor devices in the inverter are ideal.
d. Iron losses are negligible.

Fig.1. Configuration of BLDC motor and voltage source inverter (VSI) system

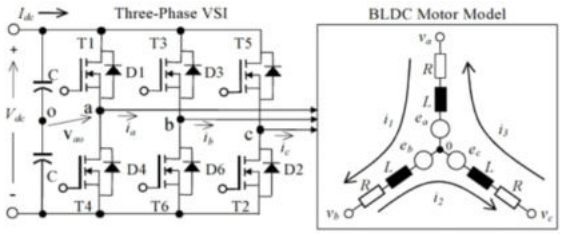

Under the above assumptions, a BLDC motor can be represented as [2]

$$\begin{bmatrix} V_a \\ V_b \\ V_c \end{bmatrix} = \begin{bmatrix} R & R & R \\ R & R & R \\ R & R & R \end{bmatrix} \begin{bmatrix} i_a \\ i_b \\ i_c \end{bmatrix} + \begin{bmatrix} (L-M) & 0 & 0 \\ 0 & (L-M) & 0 \\ 0 & 0 & (L-M) \end{bmatrix} \frac{d}{dt} \begin{bmatrix} i_a \\ i_b \\ i_c \end{bmatrix} + \begin{bmatrix} e_a \\ e_b \\ e_c \end{bmatrix} \quad (1)$$

where V_a, V_b and V_c are phase voltages, R is resistance, L is inductance, M is mutual inductance, e_a, e_b, e_c trapezoidal EMFs.

The motion equation is expressed as

$$\frac{d\omega_m}{dt} = \frac{P}{2J}(T_e - T_L - B\omega_r) \text{ and } \frac{d\theta}{dt} = \omega_r \quad (2)$$

where T_e is electromagnetic torque, T_L is load torque in Nm, J is the moment of inertia in kgm^2, B is frictional coefficient in Nm/rad, ω_m is rotor speed in mechanical rad/s. ω_r is rotor speed in electrical rad/s.
The electromagnetic torque is expressed as [3]

$$T_e = T_L + J\frac{d\omega_r}{dt} + B\omega_r \quad (3)$$

Where T_L is load torque, J is inertia, and B is damping.

Modeling And Implementation Of Bldc Motor Drive System

From Figure 2, it is clear that the proposed control system consists of two loops. The first is the current control loop that accomplishes the torque control of BLDC motor and the second loop is the speed control loop that adjusts the speed of BLDC motor. [2]
Figure 3 shows the overall block diagram of the developed model for BLDC motor drives. [2]
Fig.2. Fuzzy Logic Controlled BLDC motor drive system

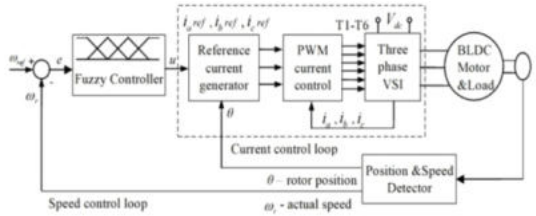

Fig.3. Simulink model of a BLDC motor.

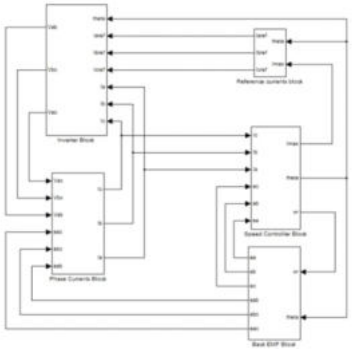

Modeling of Trapezoidal Back EMF

As shown in figure 4, the back EMF is a function of rotor position (θ) and has the amplitude $E=K_e \omega_r$ (K_e is back EMF constant), given in equation (4) and implemented as shown in figure 5. [2]

$$\begin{bmatrix} e_a \\ e_b \\ e_c \end{bmatrix} = E \begin{bmatrix} f_a(\theta) \\ f_b(\theta) \\ f_c(\theta) \end{bmatrix}, \quad E = Ke\omega r \quad (4)$$

Where $f_a(\theta)$, $f_b(\theta)$, and $f_c(\theta)$ are the Trapezoidal shape functions of rotor position with limit values between +1 and -1 defined as: [3]

$$f_a(\theta) = \begin{cases} (6/\pi)\theta & (0 < \theta \le \pi/6) \\ 1 & (\pi/6 < \theta \le 5\pi/6) \\ -(6/\pi)\theta + 6 & (5\pi/6 < \theta \le 7\pi/6) \\ -1 & (7\pi/6 < \theta \le 11\pi/6) \\ (6/\pi)\theta - 12 & (11\pi/6 < \theta \le 2\pi) \end{cases} \quad (5)$$

Fig .4. Back Emf And Phase Current Waveforms Of Bldc Motor Drive

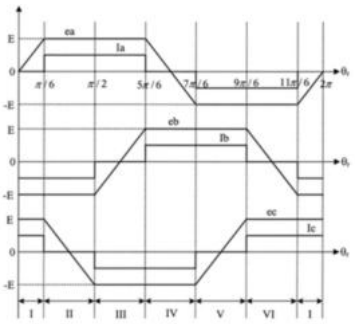

$$f_b(\theta) = \begin{cases} -1 & (0 < \theta < \pi/2) \\ (6/\pi)\theta - 4 & (\pi/2 < \theta < 5\pi/6) \\ 1 & (5\pi/6 < \theta < 9\pi/6) \\ (6/\pi)\theta + 10 & (9\pi/6 < \theta < 11\pi/6) \\ 1 & (11\pi/6 < \theta < 2\pi) \end{cases} \quad (6)$$

$$f_c(\theta) = \begin{cases} 1 & (0 < \theta < \pi/6) \\ -(6/\pi)\theta + 2 & (\pi/6 < \theta < \pi/2) \\ -1 & (\pi/2 < \theta < 7\pi/6) \\ (6/\pi)\theta - 8 & (7\pi/6 < \theta < 9\pi/6) \\ 1 & (9\pi/6 < \theta < 2\pi) \end{cases} \quad (7)$$

The electromagnetic torque is redefined using back EMF as follows:

$$T_e = (T_a + T_b + T_c) = (e_a i_a + e_a i_a + e_a i_a)/\omega_r \quad (8)$$

Substituting equations (4)-(7) in equation (8), the expression of electromagnetic torque can be defined as:

$$T_e = K_e(\ f_a(\theta) i_a + \ f_b(\theta) i_b + f_c(\theta) i_c) \quad (9)$$

Speed and Torque control

Speed and torque characteristics of the BLDC motor can be explained with equation (3), neglecting the damping factor as: [3]

$$\omega_r = \frac{P}{2J}\int (T_e - T_l)\, dt = \frac{P}{2J}\int [(T_a + T_b + T_c) - T_l]\, dt \quad (10)$$

Fig.6. Simulink diagram for speed and torque control

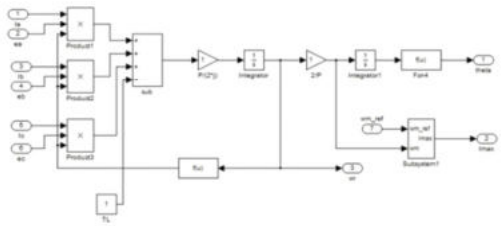

In The BLDC motor drive, duty-cycle controlled voltage pwm technique and hysteresis current control technique can be regarded as the main current control strategies. In this paper bipolar hysteresis current control is used for obtaining the fast dynamic responses during transient states. This current control method is explained based on the case of phase A. As shown in figure 7 (a), current control for phase A can be divided into each four-period following the polarity of the current: [3]

Case I: > 0

- Period 1: < Lower L imit (LL) → Switch $_1$ is turned on.
- Period 2: > Upper Limit (UL) → Switch $_1$ is turned off and $_4$ is conducted.
- Period 3: LL < < UL and T >0 → Switch $_1$ is turned on.
- Period 4: LL < < UL and T < 0 → Switch $_1$ is turned off and $_4$ is conducted.

Case II: > 0

- Period 1: > UL → Switch $_4$ is turned on.
- Period 2: < LL → Switch $_4$ is turned off and $_1$ is conducted.
- Period 3: LL < < UL and T > 0 → Switch $_4$ is turned on.
- Period 4: LL< < UL and T <0 → Switch $_4$ is turned off and $_1$ is conducted.

This hysteresis current control logic is realized in a function block f_a (u) in cooperation with the measured phase A current , current reference and rotor position as shown in Figure 7(b), such as

$$f_a(u) = (u[4] > \pi/6) * (u[4] < 5\pi/6)$$
$$\left\{\begin{array}{l} [(u[1] < u[3] * 0.9) - (u[1] > u[3] * 1.1)] \\ +[(u[1] > u[3] * 0.9) * (u[1] < u[3] * 1.1) * (u[1] > u[2])] \\ -[(u[1] > u[3] * 0.9) * (u[1] < u[3] * 1.1) * (u[1] < u[2])] \end{array}\right\}$$
$$+(u[4] > 7\pi/6) * (u[4] < 11\pi/6)$$
$$\left\{\begin{array}{l} [-(u[1] > -u[3] * 0.9) + (u[1] < -u[3] * 1.1)] \\ -[(u[1] < -u[3] * 0.9) * (u[1] > -u[3] * 1.1) * (u[1] < u[2])] \\ +[(u[1] < -u[3] * 0.9) * (u[1] > -u[3] * 1.1) * (u[1] > u[2])] \end{array}\right\} \quad (11)$$

Where u[1] is the measured I_a, u[2] is the previous value of I_a u[3] is the maximum value of current reference (I_{max}), u[4] is the rotor position (θ,), u[3]*0.9 is the lower limit and u[3]*1.1 is the upper limit.

Fig.7. (a) Hysteresis current control for phase A; (b) its implementation

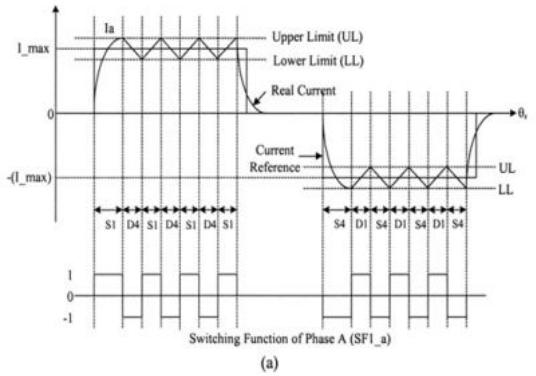

(a)

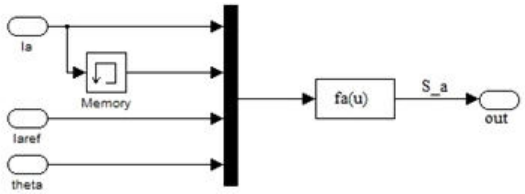

(b)

From the hysteresis block, the switching function S_a, S_b and S_c are determined to model the operation of the pwm inverter. The switching function concept is powerful tool in understanding and optimizing the performance of the static power converters/inverters. Using the switching function concept, the power conversion circuits can be modeled according to their functions, rather than circuit topologies. Therefore, it can achieve simplification of the overall power conversion functions, so that convergence and long-run time problems can be solved. [5-8]

Voltage source inverter (VSI)

As shown in Figure 1, only the two phases are excited through the conduction operating modes. Therefore, three phase currents are considered in terms of the line to line voltages. The following voltage and current equations can be obtained: [2]

$$V_{ab} = 2Ri_1 + 2(L-M)\frac{di_1}{dt} + e_{ab}$$
$$V_{bc} = 2Ri_2 + 2(L-M)\frac{di_2}{dt} + e_{bc}$$
$$V_{ca} = 2Ri_3 + 2(L-M)\frac{di_3}{dt} + e_{ca} \quad (12)$$

Where i1, i2, and i3 are loop currents, eab, ebc and eca are the line to line back EMF's:

$$e_{ab} = e_a - e_b, e_{bc} = e_b - e_c, e_{ca} = e_c - e_a$$

and the phase currents:

$$i_a = i_1 - i_3, i_b = i_2 - i_1, i_c = i_3 - i_2$$

Using the switching function $S_{a,b,c}$ which is obtained from hysteresis block, V_{ao}, V_{bo}, and V_{co} in reference to midpoint of dc supply voltage can be calculated as: [8]

$$v_{ao} = \frac{V_d}{2}S_a = \frac{V_d}{2}\sum_0^{\infty} A_n \sin(n\omega t)$$
$$v_{bo} = \frac{V_d}{2}S_b = \frac{V_d}{2}\sum_0^{\infty} A_n \sin[n(\omega t - 120)]$$
$$v_{co} = \frac{V_d}{2}S_c = \frac{V_d}{2}\sum_0^{\infty} A_n \sin[n(\omega t - 240)] \quad (13)$$

Then the inverter line to line voltages can be derived as

$$v_{ab} = v_{ao} - v_{bo}, v_{bc} = v_{bo} - v_{co}, v_{ca} = v_c - v_a \quad (14)$$

The implementations of the above-explained numerical PWM inverter voltage and current equations are shown in Figure 8 and 9.

Reference Current Generator

The motor's reference phase currents ($i_a$ref, $i_b$ref, $i_c$ref) are determined using reference current generator, by considering reference current amplitude (I_{max}), which is calculated depending on rotor position (θ). The reference current amplitude (I_{max}) can be obtained as

$$I_{max} = u/k_t \quad (15)$$

where u is the control signal obtained from fuzzy controller and k_t is the torque constant of the BLDC motor. The reference phase currents given in Table 1 can be acquired from figure 4. Figure 10 shows the Simulink diagram for reference currents. [8]

Fig.8. Generation of line-to-line inverter voltages

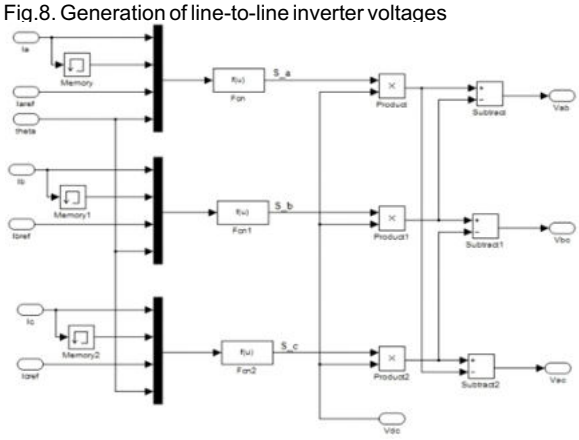

Fig.9. Simulink diagram for the three phase currents

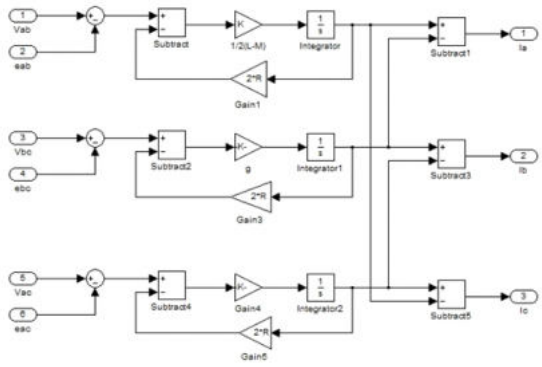

Fig.10. Simulink diagram for reference currents

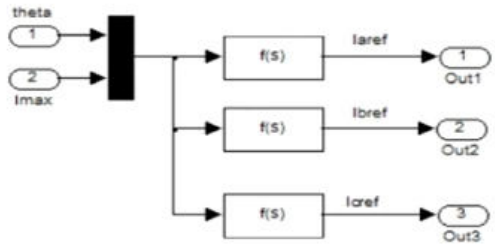

Table 1: Reference Currents of BLDC motor

Rotor position (θ-Degree)	Reference Currents (A)		
	$i_a$ref	$i_b$ref	$i_c$ref
0-30	0	$-I_{max}$	I_{max}
30-90	I_{max}	$-I_{max}$	0
90-150	I_{max}	0	$-I_{max}$
150-210	0	I_{max}	$-I_{max}$
210-270	$-I_{max}$	I_{max}	0
270-330	$-I_{max}$	0	I_{max}
330-360	0	$-I_{max}$	I_{max}

Fig.11. Structure of a Fuzzy logic controller

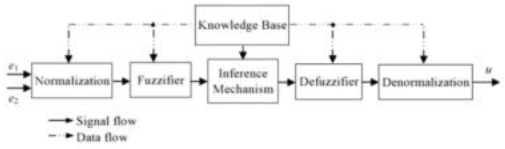

Design of Fuzzy Logic Controller (FLC)

Figure 11 shows the block diagram of FLC with two inputs (e1, e2) and one output (u). The error is calculated by subtracting the reference speed from the actual rotor speed as follows: [13]

$$e_1[n] = \omega_{ref}[n] - \omega_r[n] \qquad (16)$$

where e1[n] is the error , ωref[n] is the reference speed, and ωr[n] is the actual motor speed. The change in error is given by

$$e_2[n] = e_1[n] - e_1[n-1] \qquad (17)$$

here e_1[n-1] is the previous error value.

In the fuzzy logic control system, two normalization parameter (N_{e1}, N_{e2}) for input and one de-normalization parameter (N_u) for output are defined. In normalization process, the input values are scaled between (-1,+1) and in the de-normalization process, the output values of fuzzy controller are converted to a value depending on the terminal control element.

The fuzzy values obtained from fuzzy inference mechanism have to be converted to crisp output value (u), by de-fuzzifier process. For this purpose, the triangle fuzzy membership function is defined for each input and output values by seven clusters. Figure 12 illustrates the membership function used to fuzzify two input values (e_1,e_2) and de-fuzzify output (u) of the fuzzy controller. For seven clusters in the membership functions, seven linguistic variables are defined as: Negative Big (NB), Negative Medium (NM), Negative Small (NS), Zero (Z), Positive Small (PS), Positive Medium (PM), Positive Big (PB).[14]

Fig.12. Membership functions of Fuzzy Controller

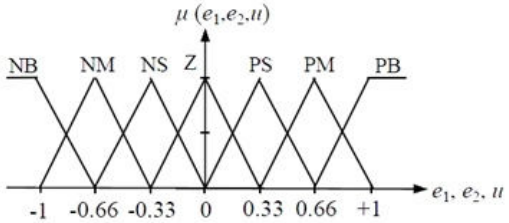

A sliding mode rule base used in FLC is given in Table 2. The fuzzy inference operation is implemented by using 49 rules. The min-max compositional rule of inference and the center-of-gravity method have been used in de-fuzzifier process.

Table 2: Rule Base for Fuzzy Controller

Input-e_1	Input-e_2						
	NB	NM	NS	Z	PS	PM	PB
NB	PB	PB	PM	PM	PS	PS	Z
NM	PB	PM	PM	PS	PS	Z	NS
NS	PM	PM	PS	PS	Z	NS	NS
Z	PM	PS	PS	Z	NS	NS	NM
PS	PS	PS	Z	NS	NS	NM	NM
PM	PS	Z	NS	NS	NM	NM	NB
PB	Z	NS	NS	NM	NM	NB	NB

Fig.13. Simulink diagram of fuzzy logic and PID controller

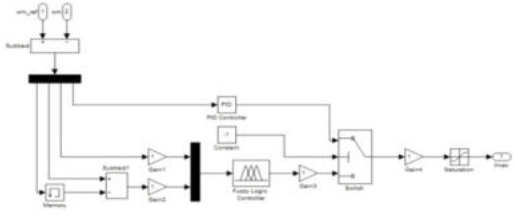

MATLAB/Fuzzy Logic Toolbox is used to simulate FLC which can be integrated into simulations with Simulink. The FLC designed is transferred to MATLAB-Workspace by the command “Export to workspace”. Figure 13 shows the Simulink diagram of Fuzzy logic and PID controller. These control algorithms can be compared by using switch block. If the mid-point of switch block is '-1', FLC is selected, and in case the mid-point of switch block is '1' PID is selected. [15, 2]

Simulation Results

BLDC motor specifications used in simulation are shown in Table 3. The Figure 14 shows the generated back EMF and the phase current waveforms from the rotor position and at operating speed of 3,500 rpm. At 3,500 rpm the rotor position is varied from 0 to 2π per electric cycle 0.017s and the amplitude is 39.36V. Also, the actual phase currents are successfully obtained by the hysteresis control algorithm, and they are well synchronized with their counterpart back EMF waveforms. [2,3]

Rating (P)	106 watt
Number of Phase	3 (star)
Rated Speed	3500 rpm
Rated current	6.8A
R	1.5Ω
(L-M)	6.1 mH
J	0.0019 Ncm-s^2
K_e	0.0419 V/rad/s
K_t	4.19 Ncm/A

Fig.14.(a)Back EMF waveforms (b) phase currents waveforms based on rotor position at 3,500 rpm

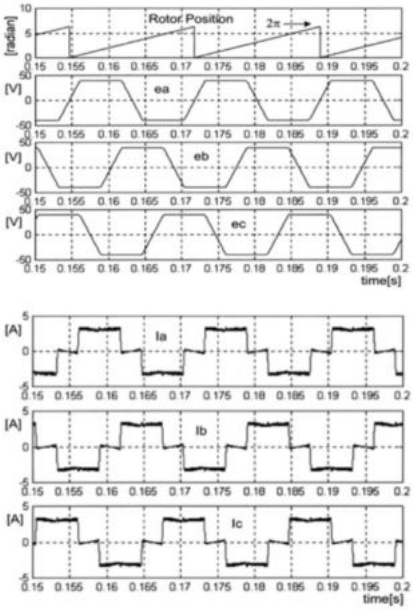

Figure 15 shows the detailed operational characteristics of PWM inverter based on the switching function concept. The switching function for the phase A, S_a is given in figure 15. In order to hold the currents to be switched between the hysteresis upper and lower bands, the switching function signals are only produced during the 120° conduction periods. The line-to-line voltage waveforms are obtained by using the switching function S_a. The produced line-to-line voltage (v_{ab}) according to the conduction modes is demonstrated in Figure 16.

Figure 17 shows the dynamic responses of the speed, torque and I_{max}, respectively. The reference value of maximum current (I_{max}) is computed from the generated constant torque reference, consequently it is used in hysteresis control block. [10-12]Furthermore, the control algorithms, FLC and PID can be compared by using developed model. As shown in Figure 18 (a) and (b), if the PID controller is used, the real speed and torque reach the desired value in 0.02s. On the other hand, if FLC is used, the real speed and torque reach the desired value in 0.15s. In conclusion it can be said that unlike the classical controller, FLC is more effective in BLDC motor drives. [15]

Fig.15. Back EMF and switching function S_a for phase A

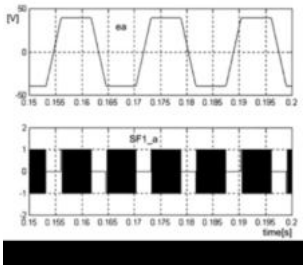

Fig.16. Phase currents and line to line inverter voltage

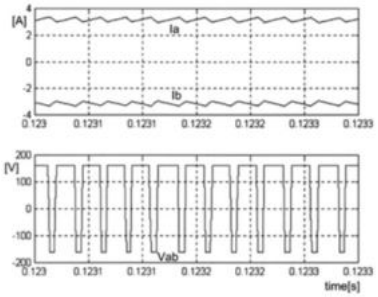

Fig.17. Electromagnetic torque, speed of BLDC motor, and maximum current (I_{max})

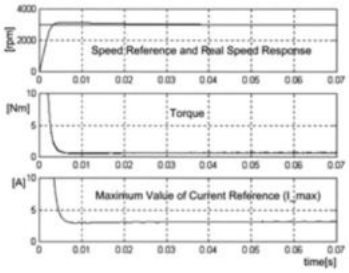

Fig.18. Comparison of PID and FLC (a) for speed (b) for torque

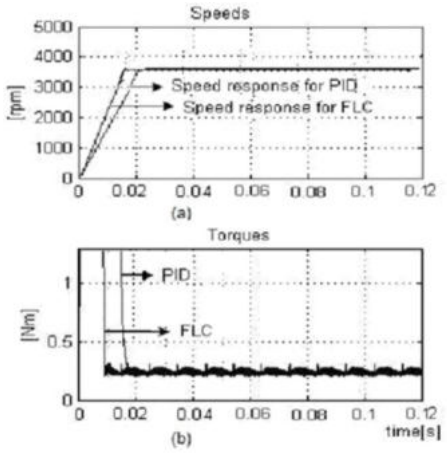

Conclusion

In this paper, a comprehensive analysis of brushless DC drive system has been performed by using fuzzy logic controller. The advanced simulation model for BLDC motor drive system is implemented under MATLAB/Simulink through which it is expected that the dynamic characteristics can be effectively monitored and predicted, so that the performance of developed system can be more precisely analyzed. Furthermore, the control algorithms, FLC and PID have been compared by using the developed model which results that the desired real speed and torque values could be reached in a short time by FLC controller. The results show that MATLAB paired with Simulink is a good simulation tool for modeling and analyze fuzzy logic controlled brushless DC motor drives.

REFERENCES

P. Yedamale, Brushless DC (BLDC) Motor Fundamentals. Chandler, AZ: Microchip Technology | M. Cunkas and Omer Aydogudu, Realization of Fuzzy Logic Controlled Brushless DC motor drives using MATLAB/SIMULINK, Mathematical and Computational Applications, Vol. 15, No. 2, pp. 218-229, 2010. | B.K. Lee and M. Ehsani Advanced Simulation Model for Brushless DC Motor Drives, Electric Power Components and Systems 31, 841868, 2003. | C. Subba Rami Reddy and M. Surya Kalavathi, Performance evaluation of hybrid fuzzy logic controller for brushless dc motor drive, International Journal of Engineering Science and Technology (IJEST), ISSN : 0975-5462, Vol. 3, No. 6 June 2011. | P. Pillay and R. Krishnan, Modeling, simulation, and analysis of permanent-magnet motor drives, part II: the brushless DC motor drive, IEEE Trans. on Industry Applications 25, 274279, 1989. | E. P. Wiechmann, P. D. Ziogas, and V. R. Stefanovic, Generalized functional model for three phase PWM inverter/rectifier converters, Proc. of the IEEE Industry Application Society Annual Meeting IAS'85, pp. 984993, 1985. | L. Salazar and G. Joos, PSPICE simulation of three-phase inverters by means of switching functions, IEEE Trans. on Power Electronics, vol. 9, no. 1, pp. 3542, January 1994. | B.K. Lee and M.A. Ehsani, Simplified functional model for 3-phase voltage-source inverter using switching function concept, IEEE Trans. on Industrial Electronics 48, 309321, 2001. | P. D. Evans and D. Brown, Simulation of brushless DC drives, Proc. of the IEE, vol. 137, no. 5, pp. 299308, September 1990. | R. Carlson, M. Lajoie-Mazenc, and C.D.S. Fagundes, Analysis of torque ripple due to phase commutation in brushless DC machines, IEEE Trans. on Industry Applications 28, 632638, 1992. | T. M. Jahns and W. L. Soong, Pulsating torque minimization techniques for permanent magnet AC motor drivesa review, IEEE Trans. on Industry Applications, vol. 43, no. 2, pp. 321330, April 1996. | S.K. Safi, P.P. Acarnley, and A.G. Jack, Analysis and simulation of the high-speed torque performance of brushless DC motor drives, Proc. of the IEE 142, 191200, 1995. | Zadeh, L.A. (1965): Fuzzy sets in information and control, New York, Academic, Vol. 8, pp. 338-353. | CK. Lee and WH. Pang, A Brushless DC Motor Speed Control System Using Fuzzy Rules, IEE Power Electronics and Variable Speed Drives, pp.101-106, 1994. | Ali Akcayol, M., et al. (2003): An education tool for fuzzy logic controlled BLDC, IEEE Trans. on Education, Vol. 45, No. 3, pp. 33-42.